THE GAIA CONCEPT

L. Lindegren[1], M.A.C. Perryman[2]

[1] Lund Observatory, Box 43, S-22100 Lund, Sweden
[2] Astrophysics Division, ESTEC, Noordwijk 2200AG, The Netherlands

ABSTRACT

GAIA is a preliminary concept for an astrometric mission, expected to lead to positions, proper motions and parallaxes of some 50 million stars down to about $V = 15$ mag, with an accuracy of better than 10 μas, along with multi-colour multi-epoch photometry of each object. The concept involves three optical Fizeau interferometers, each with a 1° field of view, set at fixed angles to each other and scanning the sky at a rate of 120 arcsec/s. We describe some of the considerations that have gone into this concept. Accuracy estimates are given both for a baseline option, which we consider to be feasible with existing detector technology, and for a more advanced option using 'direct fringe detection', which would provide even higher accuracy and a fainter limiting magnitude.

Key words: space astrometry, interferometry, GAIA

1. INTRODUCTION

GAIA (Global Astrometric Interferometer for Astrophysics) is a preliminary concept for an astrometric mission, aiming at the broadest possible astrophysical exploitation of optical interferometry using a modest baseline length ($\sim$ 3 m). In its present form, the mission is estimated to give the positions, parallaxes and annual proper motions of some 50 million objects down to $V = 15$ mag with an accuracy of better than 10 μas (microarcsec), along with multi-colour multi-epoch photometry of each object. The general scientific objectives are reviewed in these proceedings by Perryman & Lindegren (1995).

The term 'global' puts emphasis on a particular quality of the results expected from such mission, namely that of covering a very large number of objects scattered over the whole celestial sphere, while referring all results to unique and well-defined measurement systems. For the astrometry, in particular, this implies the determination of absolute parallaxes and of a dense and undistorted optical reference frame for positions and proper motions. But the principle applies equally to the photometric results, where globality is essential, for example, for variability studies and accurate calibration of physical stellar parameters. The Hipparcos mission was global in this sense, and GAIA will extend the principle on a vastly more ambitious scale by the introduction of interferometry and modern detectors.

From a technical viewpoint, the general principles of the GAIA concept can be summarised in the following points:

- It is a continuously scanning instrument, capable of measuring simultaneously the angular separations of several hundred star images as they pass across a field of view of about 1° diameter. Simultaneous multi-colour photometry of all astrometric targets is a necessary and integral part of the concept.

- High angular resolution in the scanning direction is provided by optical interferometry on a baseline of $\sim$ 3 m. The large field of view implies the use of Fizeau type interferometers.

- The wide-angle (global) measuring capability is realized by means of two or more interferometers mechanically set at large angles to each other and scanning the same great circle on the sky. The precise 'basic angles' between the interferometer baselines are determined from the 360° closure condition on each great-circle scan. Short-term (< 3 hours) variations are passively controlled and, if necessary, monitored by internal metrology.

- The whole sky is systematically scanned according to a pattern which permits, after some years of scanning, a complete determination of the astrometric stellar parameters along with attitude and (time-variable) instrument parameters. All parameters are in principle determined in a single, global adjustment procedure.

Within this general outline a multitude of options exist which remain to be explored, optimised and weighed against each other. These include, for instance, the number and optical design of the Fizeau interferometers, choice of wavelength bands, detection systems, basic angles, metrology system, satellite layout, and orbit. This paper describes a technically reasonable *baseline configuration* (Lindegren & Perryman 1994) which would achieve the main mission goals as summarised above. Its main characteristics are as follows: three identical Fizeau interferometers stacked on top of each other in a cylindrical body intended to fit into a dual-launch Ariane 5 envelope, pointed at fixed angles with respect to each other; each interferometer consisting of two 50 cm (or larger) aperture mirrors, with a baseline length of $\simeq$ 2.5 m, and equipped with modulating grids and CCD detectors in the focal plane assembly.

A mission length of 5 years is proposed. Although the basic astrometric parameters (position, parallax and proper motion) can be fully disentangled in a couple of years, some of the more complex motions cannot be properly explored on a such a short time scale. This concerns,

Proceedings of a joint RGO-ESA Workshop on Future Possibilities for Astrometry in Space, *Cambridge, UK, 19-21 June 1995* (ESA SP-379, September 1995)

in particular, many binaries with periods up to several years, and the detection of possible planetary and brown dwarf companions. A survey instrument like GAIA is ideal for planetary detection, through its screening of a very large number of stars for their photocentric motions (Lattanzi, Casertano & Perryman 1995a,b), but measurements extending over a significant fraction of the orbital period are mandatory.

Compared with Hipparcos, the dramatic increase in accuracy (100×) and number of stars (500×) is considered achievable mainly as a result of the following improvements: (a) increased optical baseline, from 0.3 m to 2.5 m; (b) increased detector efficiency (going from a photon-counting image dissector tube to a CCD); (c) multiplexed rather than sequential observations, resulting in increased observing time for target stars and the possibility to observe all stars down to the instrument's sensitivity limits.

GAIA was proposed (Lindegren et al. 1993b) as a concept for a cornerstone mission within the European Space Agency's 'Horizon 2000 Pluso scientific programme. The concept developed from the experiences of the Hipparcos project and the realization that astrometry is probably the scientifically most worthwhile application of space-borne interferometry on a short baseline. The first embryonic idea for a scanning Fizeau interferometer, due to A. Labeyrie, was contained in a proposal for a non-interferometric astrometry mission called Roemer (Lindegren et al. 1993a).

2. GENERAL DESIGN CONSIDERATIONS

This section outlines a number of considerations on a future space astrometry mission which have lead to the present baseline concept for GAIA.

2.1. Why A Scanning Instrument?

In contrast to point-and-stare missions as exemplified by the Hubble Space Telescope and the OSI and POINTS astrometry projects, the observation mode adopted for GAIA is based on continuous sky scanning. The rationale for this particular choice, which deeply affects nearly all technical, operational and scientific aspects of the mission, may be summarised as follows: (a) it follows a proven concept, namely that of the Hipparcos mission; (b) it is well suited for a global, survey-type mission with very many targets; (c) astrophysical research primarily oriented towards the physics of stars and of the Galaxy as a whole is best served by a survey-type mission encompassing large and well-defined samples of a wide variety of objects; (d) from a technical viewpoint, a continuously scanning satellite appears to be particularly efficient, and perhaps optimal, in terms of instrument stability and calibration, and observing time utilisation. This is due to factors such as the constant geometry with respect to the sun for the proposed scanning pattern; that critical instrument parameters such as the basic angle, scale value and geometrical field distortion are obtained from the closure conditions on each complete rotation of a few hours; that these calibrations are part of the normal observations and therefore do not require any overhead time; that no overhead is required for re-pointing the telescope; and that many objects are observed strictly simultaneously.

The interferometers are considered to scan the whole sky according to a pre-defined pattern similar to the 'revolving scanning law' used with Hipparcos. Thus, the axis of rotation (perpendicular to the viewing directions and interferometer baselines) is kept at a nominally fixed angle ξ from the sun, and describing a precessional motion about the solar direction at constant speed with respect to the stars. For Hipparcos the solar angle was $\xi = 43°$, but a slightly larger value (e.g., $55°$) should be adopted for GAIA for improved uniformity of sky coverage. The spin period is about 3 hours, corresponding to a speed of 120 arcsec/s for the motion of star images across the field. The spin axis must be controlled to follow the nominal scanning law to within a few arcminutes in order to guarantee sufficient overlap between successive great-circle scans.

2.2. Resolution And Astrometric Precision

The 'resolution' of an optical interferometer of baseline $B \simeq 3$ m is of the order of $\lambda/B \simeq 40$ mas. How is it possible to do microarcsec astrometry with an instrument of such modest resolution? The answer is: use a lot of photons.

The ultimate accuracy with which we can determine the direction to a point source of light is set by the dual nature of electromagnetic radiation, namely as waves (causing diffraction) and particles (causing a finite signal-to-noise ratio in the detection process). For an interferometer consisting of two (small) apertures separated by the distance B, the fundamental limit for the directional accuracy perpendicular to the fringes is given by:

$$\sigma \geq \frac{\lambda}{2\pi B\sqrt{N}} \qquad (1)$$

where λ is the wavelength and N the number of detected photons (Lindegren 1978). Given that $N \propto D^2$, where D is the diameter of each aperture, it follows that $\sigma \propto (BD)^{-1}$, and that the product BD should in general be maximised subject to the various constraints on size, mass and complexity. While a detailed trade-off must await further technical studies we have adopted $B = 2.45$ m and $D = 0.55$ m as representing a plausible interferometer compatible with the Ariane 5 launcher capabilities.

Equation (1) gives the limiting accuracy of a single angular measurement in the instrument frame. The positions, proper motions and trigonometric parallaxes of all the objects are eventually determined (in principle) by a least-squares combination of all such measurements collected over the whole mission. The accuracy of, say, the parallax of an individual star depends on the total weight of the measurements of the star, and a certain numerical factor determined by the geometry and temporal distribution of the measurements. For the parallax accuracy we may write, by a slight generalisation of Eq. (1):

$$\sigma_p = F\frac{\lambda_{\rm eff}}{2\pi BR} \qquad (2)$$

where F is a geometrical factor and R the total signal-to-noise ratio. Monte Carlo simulation of a revolving scanning law with $\xi = 55°$ gives $F \simeq 2$. Writing R instead of $\sqrt{N}$ allows the inclusion of certain other noise sources such as sky background.

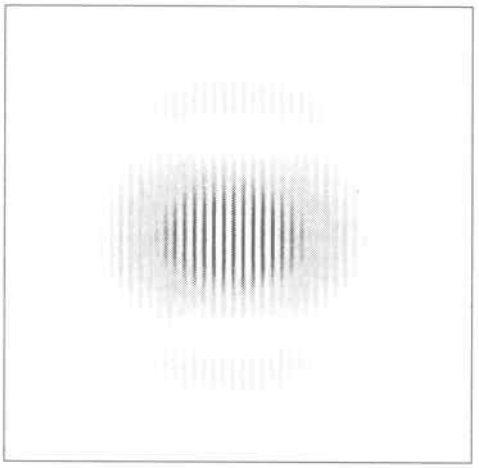

Figure 1. Calculated diffraction image of a star as produced by a Fizeau interferometer. Intensity is represented on a negative semi-logarithmic scale to show the details of the Airy pattern with superposed Young's fringes. The pupil geometry assumed for this calculation had two 0.4 m apertures on a baseline of 2.6 m. The frame is 2 × 2 arcsec. (Courtesy S. Loiseau and S. Shaklan)

For $B = 2.45$ m and $\lambda_{\rm eff} = 500$ nm we see that, in order to reach $\sigma_p \lesssim 10$ μas, we need $R \gtrsim 1000$ per object. Note that this is the required signal-to-noise ratio, on a given object, as accumulated over the five year mission.

2.3. Why Fizeau Interferometers?

Carrying on from the preceding estimates, we find, since $R \leq \sqrt{N}$, that at least some 10^6 photons need to be accumulated on a given object. At 15 mag this translates into a total integration time of $\tau \sim 1000$ s, assuming a throughput of 10 m^{2}nm. The 'throughput' is here defined as $ATQ\Delta\lambda$, where A is the collecting (aperture) area, T the total optical transmittance, Q the quantum efficiency, and $\Delta\lambda$ the wavelength bandwidth. A conservative set of numbers (for one interferometer) would be $A = 0.4$ m^2, $T = 0.5$, $Q = 0.4$ and $\Delta\lambda = 125$ nm.

Now, for a continuously scanning instrument the total time spent inside the field of view by an average object is given by:

$$\langle\tau\rangle = \frac{\Omega}{4\pi} L \qquad (3)$$

where Ω is the solid angle of the field of view and L the (effective) mission length. For $\langle\tau\rangle \sim 1000$ s and $L \sim 5$ years this gives $\Omega \sim 0.3$ deg^2 as a *minimum* field size.

Such a large field can only be realized in a Fizeau type interferometer, optically equivalent to a large (3 m diameter) telescope with two circular openings at the primary mirror. The distinguishing feature of a Fizeau interferometer (as opposed to a Michelson interferometer) is that equality of optical path length through the two apertures is maintained, throughout the field of view, by the 'underlying' telescope — provided its aberrations are small enough. In a Michelson interferometer, at least of the original type used by Michelson, the useful field is of the order of the coherence length of the light divided by the baseline, or < 1 arcsec for wideband observations on a baseline of a few metres. Adapting this principle to multi-object observation would require a separate delay line for each object. The field-of-view limitation of the classical Michelson interferometer can in principle be overcome by modifying it in such a way that the Abbe sine condition is satisfied over some finite field. However, this leads to rather complex optical solutions with no apparent advantage over the simple Fizeau principle, except when longer baselines are needed.

In summary, the use of Fizeau interferometers is a logical consequence of the adopted continuous scanning mode. The diffraction image of a star (Fig. 1) consists of the Airy disk of one of the circular pupils (radius to first minimum $= 1.22\lambda_{\rm eff}/D \simeq 0.25$ arcsec), modulated by Young's interference fringes from the two openings (fringe period $\lambda_{\rm eff}/B \simeq 0.04$ arcsec). In the absence of optical aberrations of the Fizeau interferometer this diffraction image remains the same across the whole field (isoplanatism); in other words, the fringes and the Airy disk move at the same speed when the instrument is spinning.

2.4. Spatial Resolution And Number of Pixels

The positional information is contained in the phase of the interference fringes. Let us suppose that, in order to determine the fringe phase as a function of time, we place a suitable detector directly in the focal plane of the Fizeau interferometer and record the diffraction pattern as it travels across the field of view. We call this option 'direct fringe detection'. Although very efficient in terms of photon utilisation, this option presents some considerable practical problems. First, to get a good determination of the fringe phase it is desirable to sample the diffraction pattern at least four times per fringe period, implying a pixel size of $\lesssim 10$ mas. Across a one-degree field there would then have to be at least some 360 000 pixels. (In the perpendicular direction a much lower resolution could be used, because of the smaller aperture extent normal to the baseline.) Second, the geometry of all these pixels need to be carefully calibrated in order to map the pixel coordinates of the fringes into angular measures in the field of view. Third, the combination of high spatial and temporal resolution (the latter caused by the rapid motion of the images) potentially results in a very high data rate. This last problem can however be solved by on-board data processing, or by operating the detector in a Time Delayed Integration (TDI) mode. In the case of a CCD this amounts to shifting the charge image along the CCD chip in careful synchrony with the moving optical image. TDI can be thought of as an analogue computer mapping the three-dimensional photon events (x, y, t) into a two-dimensional data stream $(t - x/v, y)$, taking advantage of the isoplanatism of the images and their known speed (v) relative to the detector.

We do not exclude that detectors of sufficient resolution and geometrical linearity will become available in the coming years as a result of ongoing or potential development programmes. Such a possibility might be offered by new developments in superconducting detectors, which provide better efficiency, broader wavelength response (into the UV and infrared), lower noise, and energy resolution (Perryman, Foden & Peacock 1993, Perryman & Peacock 1995). The possibility to adapt conventional CCD technology to direct fringe detection deserves also very careful consideration. Meanwhile, a different approach has been adopted for the baseline concept, which is considered feasible with existing technology and still achieving the nominal goals.

2.5. Use of Modulating Grids

The requirement for high spatial resolution of the detector can be dramatically relaxed by the use of modulating grids. The idea is well known from ground-based astrometry (e.g., photoelectric meridian circles) and Hipparcos: a series of slits in the focal plane modulates the transmitted star light, which is then picked up by a detector. The spatial resolution need only be some arcseconds, in order to reduce background light and isolate the star signal from that of other stars. This has two practical advantages: first, it transforms the requirement for high spatial resolution into a corresponding requirement for temporal resolution, which may be easier to satisfy. Secondly, the requirements on spatial stability, linearity and geometrical calibration now apply to the grid instead of the detector pixels, which again make them easier to satisfy. The drawback is a significant drop in efficiency compared to the theoretical limits of Eqs. (1) and (2).

In Hipparcos the modulated light was recorded by an image dissector tube (IDT) allowing just one target to be observed at a time. For GAIA, it is essential that practically *all* the several hundred targets simultaneously visible within the field of view can be observed in parallel, otherwise there would not be sufficient integration time per object. Consequently the IDT must be replaced by a detector with at least $\sim 10^3$ independent channels. The option selected for the present baseline concept is to use CCD's operated in a special mode to allow the folded light curves to build up in pixel memory (Høg 1995).

In this mode, the electric charges generated by the modulated star light are shifted back and forth on the CCD chip at precisely the (known) frequency of light modulation. In principle $2n-1$ pixels are sufficient to store n phases of the folded light curve, where n may be in the range 4 to 8. At intervals of $1/n$ of the modulation period the charge image is shifted one pixel forward, and after $n-1$ such shifts it is quickly shifted back to its original position, immediately starting the integration of the next modulation cycle. The shift frequency must be accurately matched to the actual modulation frequency of the light (depending on the grid period, the satellite rotation rate, and the image scale) to allow the light curve to be built up over many hundred modulation cycles before the whole CCD is quickly read out and the relevant samples saved. A small field lens (Fig. 2) ensures that the illumination on the CCD is stationary during this process, by imaging the two circular openings of the interferometer at fixed points on the detector.

The grid may be designed to modulate either the amplitude of the image (by means of alternatingly opaque and transparent bands, or slits, as was used for Hipparcos), or the phase (by means of a phase hologram). In both cases the light modulation at the detector can be understood as interference of the two pupil images superposed in different spectral orders, as diffracted by the grid (Lindegren et al. 1994). The phase grid is the preferred design in view of its higher efficiency (Fig. 2). In either case the grid period must match the mean fringe spacing ($\lambda_{\rm eff}/B$) in order to produce a good modulation. For the same reason it is also important that fringes are seen across the whole central Airy disk, which puts a severe constraint on the permissible level of telescope aberrations.

The latter condition also restricts the useful bandwidth of the light: the bandwidth ($\Delta\lambda$) reduces the fringe contrast as one moves away from the centre of the image, since only about $\lambda/\Delta\lambda$ fringes will be visible. To obtain fringes over the whole Airy disk thus requires that $\Delta\lambda/\lambda_{\rm eff} \lesssim D/B$. The optimum bandwidth is in fact a compromise between the number of photons and the degree of modulation obtained. Provisional calculations indicate that the standard error on the phase measurement is minimised for $\Delta\lambda/\lambda_{\rm eff} \simeq 1.1D/B \simeq 0.25$.

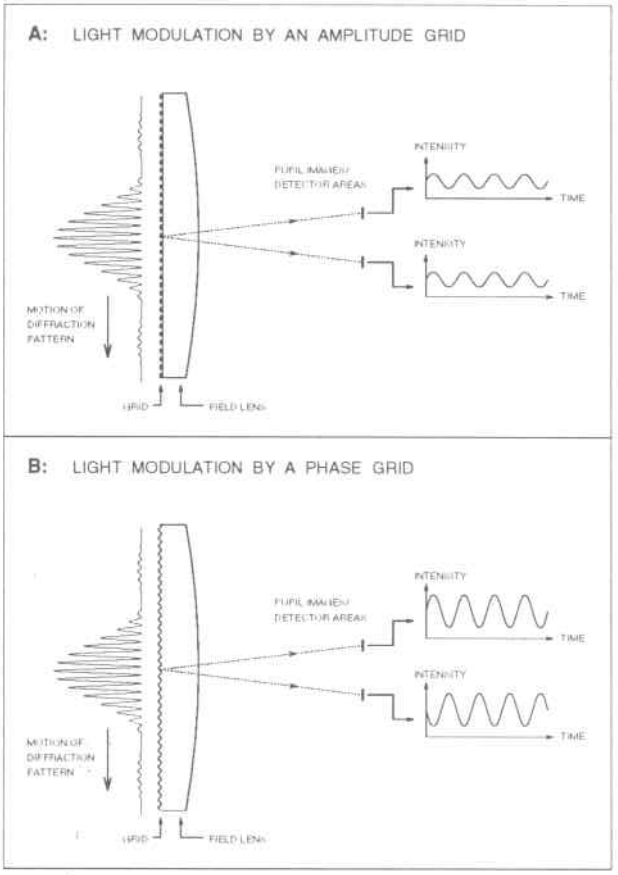

Figure 2. Principle of light modulation by an amplitude grid (a) and a phase grid (b). The phase grid transmits more light than the amplitude grid and gives deeper modulation, both factors improving the accuracy by which the fringes can be located. For the phase grid the two images of the interferometric pupils are modulated in anti-phase, requiring separate detection of the two images.

The (modest) spatial resolution needed to isolate the signals of individual stars and reduce background light may be accomplished by the field lenses indicated in Fig. 2. Each field lens defines a 'subfield' in which the signals from all sources (target star, possible companion stars, background stars and diffuse background light) are superposed. In practice a whole array of field lenslets is needed to cover a large field with such subfields. The size of a subfield should be small enough that, most of the time, there is no significantly disturbing star within that area. For instance, if we aim at a limiting magnitude of about $V = 15.5$ mag, any star brighter than $V = 16.5$ mag must be considered as a potentially serious disturber. The mean density of such stars (Allen 1973) is about 3000 deg^{-2}. For the mean probability of such a disturbance to be less than 10%, say, the subfield

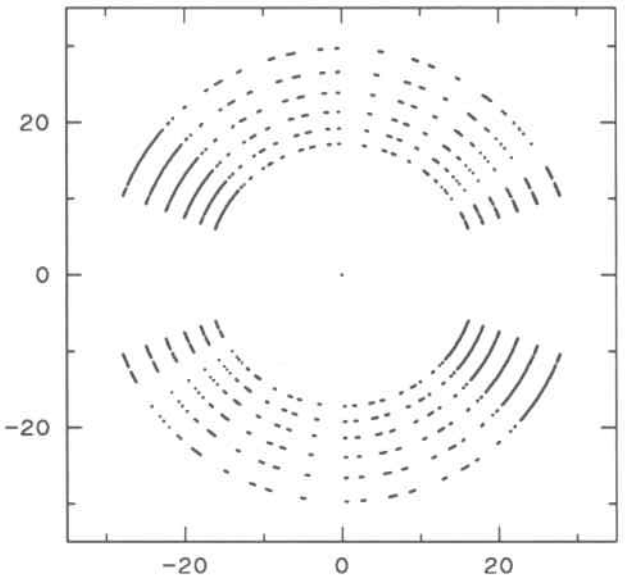

Figure 3. Typical sampling of the Fourier (uv) plane resulting from the multiple scans across a given object by grids of different periods. The axes give the spatial frequencies in cycles/arcsec in ecliptical coordinates. Aperture synthesis methods can be used to reconstruct an image consisting of moving point sources, such as a multiple star.

area must be smaller than about 400 arcsec^2. The average sky background within this area is equivalent to one star of magnitude 16: this contributes an acceptable level of photon noise but no modulation. On the other hand, the subfield cannot be made too small, since that would require to frequent readouts of the folded light curves, resulting in a lower signal-to-noise ratio, at least for CCD type detectors. It will be advantageous to make the subfields elongated in the scanning direction.

2.6. Colour Bands And Image Synthesis

One of the lessons from Hipparcos is that colour information on all astrometric targets is essential in order to to handle properly the instrument 'chromaticity'. Chromatic effects appear also in all-reflective telescopes at the sub-resolution level due to the wavelength dependence of diffraction. For GAIA a rough knowledge of target spectra will be needed for the astrometric reductions, quite apart from the scientific value of such information. Multicolour photometry must therefore be designed as an integral part of the concept.

The use of modulating grids and the pupil geometry of the interferometer imposes a natural relative bandwidth of $\Delta\lambda/\lambda \simeq 0.25$. The whole visible spectrum could be covered by about 6 such colour bands (e.g., 350–450, 400–510, 450–580, 510–650, 580–740, 650–830 nm) with a 50% overlap of successive bands in order to obtain a sufficiently dense sampling of the spectrum (Young 1994). Additional spectrophotometric information may be provided by the incoherent detectors (Sect. 2.7).

Since the grid period must match the fringe period, the colour bands mentioned above will require grids with six different periods, ranging from $s \simeq 34$ to 62 nm. Each scan across an object with a specific grid period provides information on the total intensity of the object (equal to the DC component of the modulated signal) and on the phase and amplitude of the AC component; this is equivalently given by the complex Fourier components at the three spatial frequencies $-2\pi/s$, 0, and $2\pi/s$. Measurements in the six colour bands together provide information at 13 different spatial frequencies. Since a given object is scanned in many different directions in the course of a few years, the Fourier (uv) plane of the object will be sampled in a large number of points (Fig. 3). By means of aperture synthesis methods it will be possible to reconstruct moderately complex images, e.g., consisting of several moving point sources. The use of several different grid periods will in particular make the treatment of double and multiple stars much more efficient than was the case for Hipparcos.

2.7. Incoherent Imaging Mode

Operating the telescope as a Fizeau interferometer requires that the Airy disks formed by the two 0.55 m openings add coherently to form interference fringes. This condition will certainly be met at the centre of the field and out to a certain field angle, where residual aberrations become significant. It may however be possible to construct the instrument to have an even larger (unvignetted) field, albeit with seriously reduced fringe contrast in the outer part of the field. The star images in this outer field still contains substantial astrometric information, corresponding to the resolution of the 0.55 m aperture, and of course the complete photometric information. This suggests that the outer part of the field can profitably be used in an *incoherent* imaging mode for additional astrometric and photometric measurements. The term 'incoherent' here simply means that the information is derived from the Airy envelope of the stellar images instead of the interference fringes. The theoretical loss of astrometric precision is $2B/D \simeq 9$, but in practice the loss is smaller because the direct fringe detection, using CCD's operated in the TDI mode, can be used for the incoherent imaging. The principle of operation in this mode corresponds exactly to that of a proposed non-interferometric astrometric mission, Roemer (Lindegren et al. 1993a) or Roemer+ (Høg 1994), and the predicted performance is even slightly better than for Roemer+.

The addition of the incoherent imaging mode brings about some very significant advantages and a considerable strengthening of the overall mission performance:

(a) Compared with the use of a modulating grid, the CCD directly in the focal plane gives better light economy and much more efficient suppression of background radiation and nearby images, resulting in a fainter limiting magnitude ($V = 20$), albeit at a reduced accuracy.

(b) The wavelength passbands for the incoherent mode can be chosen quite freely to serve a number of different purposes, including intermediate and narrow bands selected for astrophysical reasons, such as Strömgren and Hβ photometry to $V \sim 16$ mag.

(c) The incoherent imaging mode provides attitude information needed both in real time, for the operation of the detectors, and *a posteriori*, as required for proper interpretation of the coherent measurements in the data reductions.

(d) Positions determined by the incoherent imaging can be used as starting points for a solution based on the interferometric data. This brings the latter solution into the linear regime (phase errors $\ll 1$ rad), allowing considerable simplification of the processing and eliminating possible ambiguities and spurious solutions.

(e) The CCD detectors surrounding the interferometric field can be used for coarse focussing and control of mirror alignments, since the star images from the two pupils must overlap completely and in all parts of the field when the mirrors are correctly adjusted. Since this function does not depend on the formation of fringes, it should be particularly useful for the first phase of fringe acquisition.

(f) Finally, the incoherent imaging mode provides a reliable and useful 'backup' facility in a scenario where one or more of the interferometers, for some technical reason, fails to produce fringes. In such a case the interferometric detectors do not produce any astrometrically useful data at all, whereas the incoherent mode still provides photometry at nearly the full accuracy and astrometry certainly at the sub-milliarcsec level.

3. CURRENT BASELINE DESIGN FOR GAIA

Based on the preceding considerations, a provisional design for GAIA has been outlined which appears technically feasible with current or foreseeable technology, and which would achieve the main mission goals summarised in the Introduction. This section provides a brief specification of its main elements, including accuracy estimates.

In a sense, the concept identified here may be considered as a 'minimum' mission. If considered appropriate, technological developments could permit enhanced scientific performances: in particular we may identify the following as areas in which improvements might occur: (i) improved (more efficient, energy sensitive) detectors, including detectors sensitive in the near infra-red and suitable for direct fringe detection; (ii) enlarged optical elements (if, for example, mirror weights can be decreased); (iii) longer interferometric baselines (if, for example, a large stable deployable structure could be foreseen).

3.1. Fizeau Interferometers

As indicated in Sect. 2.3, a field of view size of the order of 1° is needed in order to accumulate sufficient integration time on each object. This implies that each interferometer is of the Fizeau type, i.e., optically equivalent to a single large telescope with two openings in the entrance pupil. The non-illuminated parts of the mirrors are removed, and we are basically left with two off-axis telescopes with a common focus.

In a first approximation we have considered the optical characteristics of the single 'underlying' 3 m telescope. An effective focal length of 10–15 m is desirable for a convenient linear size of the field (a few tens of cm). Diffraction-limited imaging over a large field implies good correction for spherical aberration, coma and astigmatism, which suggests a three-mirror system. Very preliminary optimisation of such a system led to a design whose main parameters are given elsewhere (Lindegren & Perryman 1994, Loiseau & Shaklan 1995). The mirror diameters are calculated for an unvignetted field of ±0.8°. The resulting Fizeau system is shown in Fig. 4.

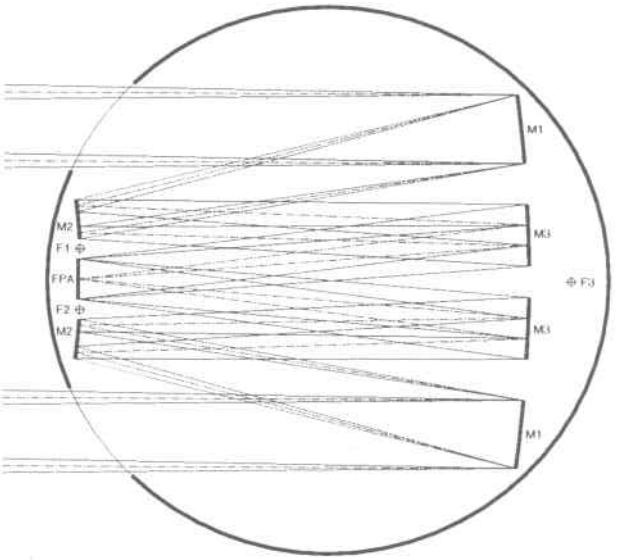

Figure 4. Optical outline of one of the Fizeau interferometers. It is optically equivalent to a three-mirror telescope (M1, M2, M3) preceded by a double aperture. FPA = focal plane assembly. F1, F2, F3 indicate three fiducial points for controlling the mirrors and focal plane assembly (see text). This configuration results from a ray-tracing solution using the Code V package (Loiseau & Shaklan 1995).

The nominal performance of the three-mirror telescope is diffraction limited within a field radius of about 0.45°. The outer part of the field, between $\simeq$ 0.5° and 0.8° radius, is still unvignetted and the geometrical images still very small; consequently this part of the field can be used for the incoherent imaging.

The Fizeau interferometer 'cut out' from this telescope would have two openings of 0.55 m diameter, with a central separation (baseline) of 2.45 m. The interferometer fits into a circular envelope of 4.4 m diameter, with the focal plane assembly conveniently located near the envelope for passive cooling of the detectors. The layout permits internal baffling so that, for instance, the tertiary mirror is invisible from the outside. Three identical interferometers (A, B, C) are stacked on top of each other in a cylindrical envelope, with baselines set at different angles. These angles should be carefully chosen so that any two interferometers, or all three of them, can be used to perform wide-angle measurements (Makarov et al. 1995). A possible set of angles would be 54° (A–B), 78.5° (B–C), and 132.5° (A–C).

3.2. Alignment and Stability Requirements

For diffraction-limited performance the relative positions of all mirror elements need to be controlled, passively or actively, to within a fraction of a wavelength. In particular the superpositioning of the Airy disks from the two circular openings must be achieved over the whole one-degree field, which puts very stringent demands on the symmetry of the system. However, not all degrees of freedom need to be controlled to the same accuracy, and passive means should be used whenever possible. For instance, it would seem likely that the focal plane assembly and the two secondary mirror segments (M2) can be con-

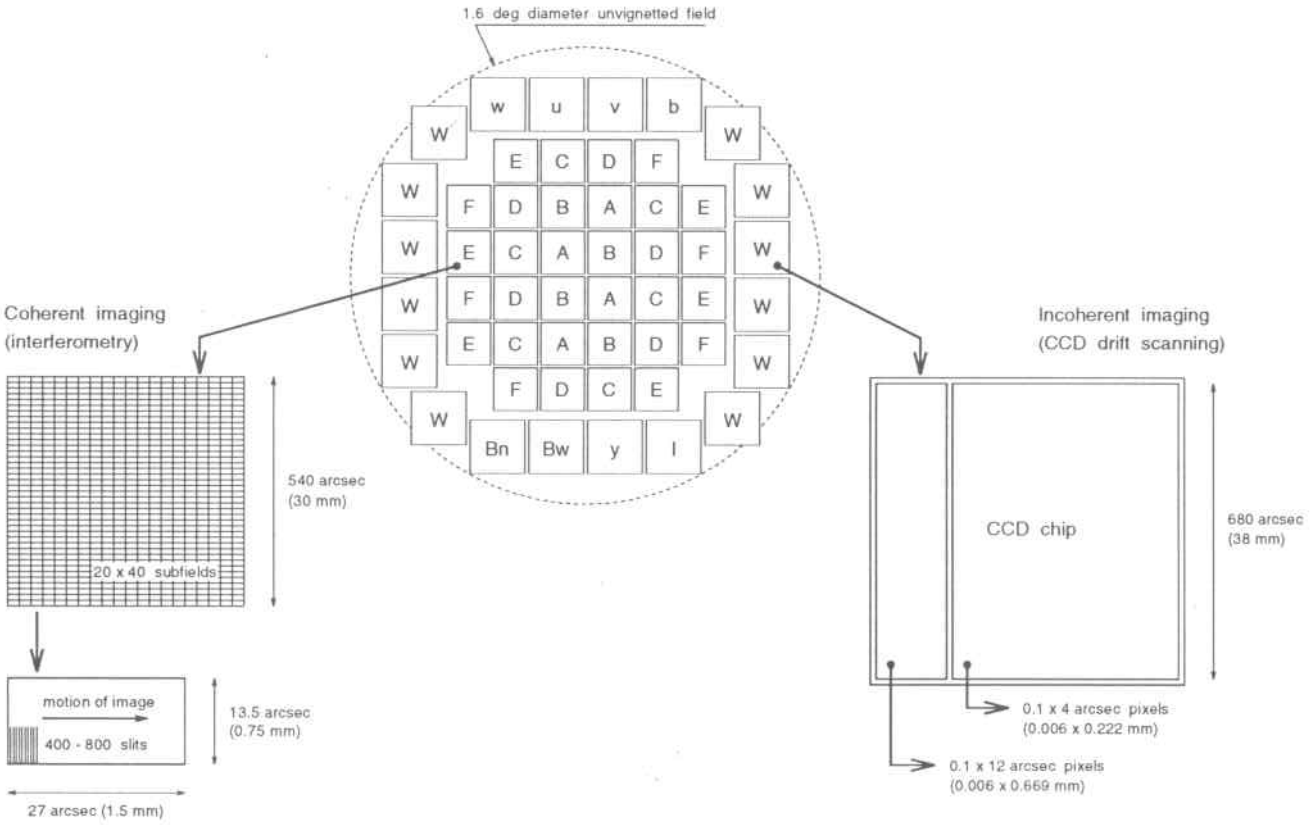

Figure 5. Schematic layout of grids and detectors in the focal plane. The inner part of the field, used in the interferometric (coherent) mode, is covered by a mosaic of phase grids, using different passband filters (A, B, ..., F) and a separate CCD behind each grid. The grids are divided in subfields with field lenses as shown in Fig. 2. The outer part of the field is used for incoherent imaging, using CCD detectors placed directly in the focal plane and operated in Time Delayed Integration mode. The detectors labelled w, u, v, b, y, I, Bw and Bn are preceded by colour filters for intermediate and narrow band photometry. Each CCD has a two regions that are read out separately to increase the dynamic range. The pixels are long and narrow.

trolled as a single unit. The other mirror segments (M1 and M3) will probably have to be actively controlled, relative to the FPA+M2 block, at least in one dimension (along the optical axis). Active control must be based on error signals that can be derived from laser gauges, but also from the focal plane detectors. The metrology requirements for the optical alignment are modest (some nm) and may be achieved with commercial gauge technique.

Much more stringent requirements are set by the stability requirements, and in particular variations of the angles between the interferometer baselines (the basic angles). While variations on time scales longer than a few hours (equal to the rotation period of the spinning satellite), as well as the absolute values of the basic angles, can be deduced from the closure conditions on each complete great-circle scan, all significant short-term variations must either be eliminated or monitored by the metrology system. On a 3-m baseline, 5 μas corresponds to a linear shift of one end by 70 pm. Thus, monitoring at the 10–50 pm precision level is likely to be required, but only for *variations* occurring on time scales up to a few hours. The basic feasibility of differential laser gauging at the pm level has already been demonstrated in the POINTS and OSI projects (Noecker et al. 1993, Shao 1993).

The interferometer baseline orientation is defined by an arbitrary fixed point on the focal grid in combination with all the mirror elements. It can therefore be monitored with respect to three fiducial points, e.g., as indicated in Fig. 4 (F1, F2, F3), by measuring distances from these points to different parts of the mirrors and focal assembly. The basic angle can then in turn be monitored from the distances of the fiducial points of one interferometer with respect to the other.

3.3. Focal Plane Assembly

Figure 5 shows a possible layout of the focal field. The inner part of the field, dedicated to the interferometric measurements (or *coherent imaging*), is covered by a mosaic of 32 grids matched to the fringes in six different wavelength bands, as discussed in Sect. 2.6. Each grid is equipped with its own CCD detector to record the resulting light modulations behind the grid. The grid is divided into subfields of 27×13.5 arcsec^2 to limit the background light and confusion from other stars, each subfield corresponding to a field lenslet as shown in Fig. 2. The wavelength passbands are implemented by filters inserted between the field lenslets and the CCD chip, with the same filter covering a whole CCD.

Table 1. Astrometric performance of GAIA in its interferometric (coherent imaging) mode, using a modulating grid (baseline) and with a hypothetical high-resolution detector (direct fringe detection). Stars of spectral type G0 have been assumed, and a mission length of 5 years. A dash means that the star is too faint to be measured against the background within the 27 × 13.5 arcsec^2 subfield assumed for the baseline option. Units: mas for parallaxes (p), mas/yr for proper motions (p.m.).

V	Baseline option		Direct fringe detection	
	p	p.m.	p	p.m.
[mag]	[mas]	[mas/yr]	[mas]	[mas/yr]
10	0.002	0.001	<0.001	<0.001
12	0.003	0.002	0.001	<0.001
14	0.006	0.004	0.002	0.001
15	0.011	0.006	0.003	0.002
16	0.020	0.012	0.005	0.003
18	–	–	0.012	0.007
20	–	–	0.030	0.018

The multiple shifting back and forth of the charges requires a high charge transfer efficiency, but should be quite feasible with current performance figures. A similar use of multiple hidden, fast image buffers on a CCD chip is proposed for the second generation of the Zurich Imaging Stokes Polarimeter (ZIMPOL II, Stenflo, Keller & Povel 1992). Alternative detectors such as photon-counting avalanche photodiodes (APD) should also be considered in conjunction with a modulating grid. Although not yet available in arrays, commercially available discrete APD detectors have characteristics that are very well suited for the present application (size of sensitive area, high quantum efficiency over a very wide spectral range, low dark counts with moderate cooling, and high time resolution). The possible advantages of the more speculative superconducting tunnel junction detectors have already been noted.

The outer part of the unvignetted 1.6° field includes a number of CCD detectors (20 as sketched in Fig. 5) placed directly in the focal plane and operated in the Time Delayed Integration (TDI) mode. The pixel width, 6 μm = 108 mas, is matched to the size of the Airy disk of the 0.55 m pupils ($1.22\lambda/D$ = 160 to 360 mas) but completely damps out any interference fringes (period λ/B = 30 to 65 mas). Some of the CCDs are equipped with intermediate and narrow-band colour filters, e.g., corresponding to a modified $uvby\beta$+I system. These provide accurate and astrophysically important photometric information on all stars observed by the interferometer and for selected fainter stars. The remaining CCDs have no filters, and are used for complementary astrometric measurements and for attitude determination and coarse mirror control.

3.4. Accuracy Estimates

For the interferometric (coherent) mode, the light modulation recorded by the detectors can be evaluated by integrating the intensity over the relevant detector area, and with respect to λ weighted by the stellar photon flux, instrument and filter transmittances, and detector quantum efficiency. Such calculations have been carried out using realistic assumptions on all instrumental characteristics. The accuracy of the phase determination, and hence on the angular coordinate of the star in the scanning direction, is then computed for a maximum likelihood estimator. The resulting errors are finally transformed into global astrometric errors by assumptions similar to those used for the Hipparcos accuracy assessment. Results of a preliminary accuracy assessment are given in the first three columns of Table 1 ('baseline option').

Table 2 gives the photon statistical limits on the astrometric and photometric precisions achievable in the incoherent imaging mode. The actual accuracy will be lower depending on how well the geometric and photometric properties of the CCDs can be calibrated, and how stable they are on time scales up to several weeks (the time period needed to achieve a complete mapping of irregularities). However, photometric accuracies better than 0.01 mag should be obtained for all survey stars ($V < 15.5$ mag), as well as sub-mas astrometric accuracy for many more fainter stars.

The columns in Table 1 headed 'direct fringe detection' refer to a hypothetical detector with sufficient spatial resolution to replace the modulating grid, as discussed in Sect. 3.5. In this option we assume a detector with similar characteristics as a CCD, except that the pixel width in the scanning direction is much smaller than the fringe period, say < 0.5 μm. As indicated by the table, this would dramatically enhance the performance both in terms of accuracy and limiting magnitude. While the use of a modulating grid is considered feasible with existing technology, and therefore retained as the baseline option, we wish to emphasize that it does not fully utilise the potential of the interferometric method. Serious consideration should therefore be given to alternative detection methods which may become feasible in the near future. The inclusion of the 'direct fringe detection' option in Table 1 may serve as an illustration of the improvement that could result from using a nearly optimal detector.

3.5. Other Mission Characteristic

The principal spacecraft characteristics needed to accommodate the identified goals are summarised as follows:

Orbit: the satellite could be operated in geostationary orbit, or at the Earth-Moon triangulation libration point L5; the advantages of the latter (Companys et al. 1993) include a reduced particle radiation background, and absence of eclipses; but operation at L5 would demand at least two ground stations, and X-band for telemetry transmission. Additional considerations are given by Flury (1995).

Data Rate: a telemetry data rate of several hundred kbits/sec is foreseen.

Mass: first estimates indicate a payload mass of below 600 kg, a bus mass of 700–800 kg, a bi-propellant fuel mass of between 600 kg (L5) and 1100 kg (geostationary orbit); giving a total launch mass of between 2100–2700 kg.

Power: the payload and total spacecraft power requirements are estimated at around 400 W and 1100 W respectively.

Table 2. Predicted mean errors in astrometry and photometry for GAIA in its incoherent imaging mode (using the outer part of the field of view). Only photon and readout noise has been taken into account. Stars of spectral type G0 have been assumed, and a mission length of 5 years. A dash means a signal-to-noise ratio ≤ 2.0 on a single CCD crossing. Filter and CCD characteristics are given at the bottom. Units: mas for parallaxes (p), mas/yr for proper motions (p.m.), and milli-magnitudes for the photometry (calculations kindly provided by E. Høg).

	Astrometry		Photometry [milli-mag]								
V [mag]	p [mas]	p.m. [mas/yr]	W	w	u	v	b	Bn	Bw	y	I
8	0.002	0.002	0.1	0.5	0.3	0.1	0.1	0.3	0.1	0.1	0.1
10	0.003	0.002	0.1	1.2	0.7	0.3	0.2	0.7	0.2	0.2	0.1
12	0.008	0.005	0.1	3.0	1.8	0.8	0.6	1.7	0.6	0.6	0.3
14	0.020	0.011	0.1	7.8	4.5	2.0	1.4	4.2	1.4	1.4	0.6
16	0.05	0.03	0.3	22.5	12.1	5.0	3.7	11.1	3.7	3.7	1.6
18	0.14	0.08	0.7	–	44.1	14.0	10.1	39.6	10.1	10.1	4.3
20	0.5	0.3	2.2	–	–	–	38.5	–	38.5	38.8	14.2
Central wavelength [nm]			–	320	350	411	467	486	486	547	800
Filter FWHM [nm]			–	20	30	25	25	3	25	25	140
Peak transmission			–	0.30	0.40	0.60	0.70	0.70	0.70	0.70	0.96
QE of CCD			–	0.64	0.68	0.74	0.78	0.78	0.78	0.76	0.62

Deployable elements: these would include only a second antenna to ensure omnidirectional RF coverage, and (possibly) the solar panels (arranged so as to minimise the dynamical perturbations due to solar radiation pressure).

Thermal control: each interferometer would be contained within an actively-controlled thermal environment to ensure geometric stability. The CCDs at the focal surface are specifically arranged to lie close to the outer surface of the spacecraft (Fig. 4) to allow passive cooling to deep space.

4. COMPARISON WITH OTHER MISSIONS

The success of Hipparcos, and the resulting resurgence of interest in the astrophysical capabilities of astrometry, has led to a variety of recent proposals for space missions dedicated to astrometry. These missions are divided into two categories: those that aim for Hipparcos-type accuracy on a comparable number of stars (i.e., some one hundred thousand objects); and those that aim for a significantly higher astrometric accuracy.

In the former category are three proposed missions from scientists within the former Soviet Union (Lomonosov, Regatta-Astron, and AIST). These have been under consideration for several years, are still in the study phase, and all face uncertain financial support. The objectives of all three missions was to achieve Hipparcos-type (milliarcsec) accuracy on up to a few hundred thousand stars, taking the Hipparcos goals as roughly indicative of the state of the art. Their scientific importance was based on maintaining the reference frame established by the Hipparcos mission throughout the coming decades—the optical reference frame defined by Hipparcos will degrade with time as a result of the uncertainties on the individual proper motions, such that a mission in 10–20 years from now, with individual accuracies in the range 1–2 mas will still have a useful and important, if not fundamentally new, scientific value.

Very recently, a Japanese Astrometric Satellite has been mentioned (Yoshizawa, private communication). This is at an early study phase only, no details have been made available, but it is considered to lie within the same type of mission concept as those described in the previous paragraph.

Significantly higher astrometric accuracy is the goal of the JPL's OSI and SONATA concepts (Shao 1993, Buscher et al. 1995), the proposed POINTS mission (Reasenberg et al. 1994a), and a recently proposed low-cost alternative NEWCOMB (Reasenberg et al. 1994b). These programmes aim to reach accuracies at the level of a few μas or better, per observation, with some or all of these *pointed* (rather than scanning) instruments being able to benefit, in a similar way to GAIA, from repeated measurements throughout the mission. Thus the limiting magnitude of POINTS is between 14–18 mag depending on adopted mission concept, NEWCOMB currently aims to reach an accuracy of about 100 microarcsec in a single measurement of about 4 min, OSI's target is 5 microarcsec accuracy on 20 mag stars, while SONATA is targetting 0.5 microarcsec for 14 mag objects after 4 hours. However, being pointed rather than scanning instruments, these proposed missions are able to contain only a relatively small target observing list, of say several hundred, or several thousand, pre-selected programme stars. Their high intended accuracy makes these programmes highly interesting for specific scientific goals (such as the detection of sub-solar mass planetary companions around selected nearby stars); however, the relatively few objects which can be observed, and their (generally) relatively bright limiting magnitude, means that these missions do not significantly overlap with, and therefore do not duplicate, the majority of the scientific goals attainable by GAIA.

For completeness, we note that there is a continuing effort to develop ground-based optical interferometers, especially in the USA, building on the success of the Mk III optical interferometer (see, e.g., Hummel et al. 1994). These instruments should ultimately provide very high relative astrometric accuracy on bright double or multiple systems; they are not seriously being considered as tools for large-angle (positional) astrometry, which is now considered to be mandatory for the large-scale determination of parallaxes and proper motions.

5. CONCLUSION

Building on the Hipparcos experiences, we have shown how global astrometry at the 10 μas level (or better) can be achieved for tens of millions of stars, using interferometry on baselines of a few metres. Initial system studies indicate that such a mission could be comfortably accommodated within the (dual-launch) Ariane 5 envelope, and within the financial envelope of the ESA cornerstone missions. The GAIA mission would be a first in space interferometry, would continue recent progress in an important scientific discipline, and seems to involve an acceptable balance between overall feasibility and required technological development.

REFERENCES

Allen, C.W., 1973, *Astrophysical Quantities*, Athlone Press (3rd edition)

Buscher, D., et al. 1995, Appl Opt, 34, 1081

Companys, V. et al. 1993, Proc. 44th IAF Congress, Graz.

Flury, W., 1995, *Orbit options for an interferometric astrometry mission*, ESA SP–379, this volume

Høg, E., 1994, In E. Høg and P.K. Seidelmann (eds.), *Astronomical and Astrophysical Objectives of Sub-milliarcsecond Optical Astrometry*, IAU Symp. No. 166, in press

Høg, E., 1995, *Some designs of the GAIA detector system*, ESA SP–379, this volume

Hummel, C.A. et al. 1994, Astron. J., 108, 326.

Lattanzi, M., Casertano, S., Perryman, M.A.C., 1995a, Boulder Workshop on 'Detection and Study of Extra-Solar Terrestrial Planets', May 1995, in press

Lattanzi, M., Casertano, S., Perryman, M.A.C., 1995b, ESA SP–379, this volume

Lindegren, L., 1978, In F.V. Prochazka and R.H. Tucker (eds.), *Modern Astrometry*, IAU Coll. No. 48, p. 197

Lindegren, L., Perryman, M.A.C., 1994, internal report submitted to the ESA Horizon 2000+ Survey Committee

Lindegren, L. (ed.), Bastian, U., Gilmore, G., Halbwachs, J.L., Høg, E., Knude, J., Kovalevsky, J., Labeyrie, A., van Leeuwen, F., Pel, J.W., Schrijver, H., Stabell, R., Thejll, P., 1993a, *Roemer: Proposal for the Third Medium Size ESA Mission (M3)*, Lund Observatory

Lindegren, L., Perryman, M.A.C., Bastian, U., Dainty, J.C., Høg, E., van Leeuwen, F., Kovalevsky, J., Labeyrie, A., Mignard, F., Noordam, J.E., Le Poole, R.S., Thejll, P., Vakili, F., 1993b, *GAIA — Global Astrometric Interferometer for Astrophysics*, proposal for a Cornerstone Mission concept submitted to ESA in October 1993

Lindegren, L., Perryman, M.A.C., Bastian, U., Dainty, J.C., Høg, E., van Leeuwen, F., Kovalevsky, J., Labeyrie, A., Loiseau, S., Mignard, F., Noordam, J.E., Le Poole, R.S., Thejll, P., Vakili, F., 1994, In J.B. Breckinridge (ed.), *Amplitude and Intensity Spatial Interferometry II*, SPIE Conference Proceedings, Vol. 2200, p. 599

Loiseau, S., Shaklan, S., 1995, SPIE Symp. *Spaceborne Interferometry II*, Orlando, in press

Makarov, V.V., Høg, E., Lindegren L., 1995, Experimental Astronomy, in press

Noecker, M.C., Phillips, J.D., Babcock, R.W., Reasenberg, R.D., 1993, In R.D. Reasenberg (ed.), *Spaceborne Interferometry*, SPIE Conference Proceedings, Vol. 1947, p. 174

Perryman, M.A.C., Foden, C.L., Peacock, A., 1993, Nucl. Instr. Methods A, 325, 319

Perryman, M.A.C., Lindegren, L., 1995, *The Scientific Goals of GAIA*, ESA SP–379, this volume

Perryman, M.A.C., Peacock, A., 1995, *A superconducting detector system for GAIA*, ESA SP–379, this volume

Reasenberg, R.D. et al. 1979, Astrophys. J., 234, L219.

Reasenberg, R.D., Babcock, R.W., Murison, M.A., Noecker, M.C., Phillips, J.D., Schumaker, B.L., Ulvestad, J.S., 1994a, In J.B. Breckinridge (ed.), *Amplitude and Intensity Spatial Interferometry II*, SPIE Conference Proceedings, Vol. 2200, p. 2

Reasenberg, R.D., Babcock, R.W., Phillips, J.D., Johnston, K.J., Simon, R.S., 1994b, In J.B. Breckinridge (ed.), *Amplitude and Intensity Spatial Interferometry II*, SPIE Conference Proceedings, Vol. 2200, p. 18

Shao, M., 1993, In R.D. Reasenberg (ed.), *Spaceborne Interferometry*, SPIE Conference Proceedings, Vol. 1947, p. 89

Stenflo, J.O., Keller, C.U., Povel, H.P., 1992, LEST Foundation Technical Report No. 54, Institute of Theoretical Astrophysics, Oslo

Young, A.T., 1994, A&A, 288, 683